Evidence of strong gene flow among French populations of the carrot cyst nematode Heterodera carotae

Magali Esquibet, Camille Gautier, Christophe Piriou, Eric Grenier, Sylvain Fournet, Josselin Montarry

▶ **To cite this version:**

Magali Esquibet, Camille Gautier, Christophe Piriou, Eric Grenier, Sylvain Fournet, et al.. Evidence of strong gene flow among French populations of the carrot cyst nematode Heterodera carotae. Plant Pathology, 2020, 69 (1), pp.168-176. 10.1111/ppa.13102 . hal-02457188

HAL Id: hal-02457188
https://hal.science/hal-02457188v1

Submitted on 8 Sep 2022

HAL is a multi-disciplinary open access archive for the deposit and dissemination of scientific research documents, whether they are published or not. The documents may come from teaching and research institutions in France or abroad, or from public or private research centers.

L'archive ouverte pluridisciplinaire **HAL**, est destinée au dépôt et à la diffusion de documents scientifiques de niveau recherche, publiés ou non, émanant des établissements d'enseignement et de recherche français ou étrangers, des laboratoires publics ou privés.

Evidence of strong gene flow among French populations of the carrot cyst nematode *Heterodera carotae*

M. ESQUIBET[1], C. GAUTIER[1,2], C. PIRIOU[1], E. GRENIER[1], S. FOURNET[1§] and J. MONTARRY[1§*]

[1] IGEPP, INRA, Agrocampus-Ouest, Université de Rennes 1, 35650, Le Rheu, France

[2] Centre Mondial de l'Innovation-Laboratoire de Nutrition Végétale Pôle Biocontrôle, Groupe Roullier, Saint Malo, France

[*] Corresponding author: josselin.montarry@inra.fr

[§] These authors contributed equally to this work

Short title: Strong gene flow in *Heterodera carotae*

Keywords: AMOVA, Genetic structure, Heterozygote deficit, Isolation by distance, Microsatellite markers, Migration.

Abstract The recent ban of the most efficient chemical nematicides lets growers without method to control the carrot cyst nematode *Heterodera carotae*. This phytoparasitic nematode species has a very narrow host range and causes severe crop losses in the main carrot-growing regions worldwide. The development of alternative means of management of *H. carotae* is thus essential and need knowledge about the adaptive abilities of *H. carotae*, which mainly depend on gene flow among populations. The goal of this study was to describe the genetic structure of *H. carotae* populations at the spatial scale of the main infested French carrot-producing region, i.e. Lower Normandy, and to disentangle the causes of the heterozygote deficit in this polyvoltine species. Our results, obtained thought the microsatellite genotyping of populations collected at the plant and at the field scales, showed i) that the heterozygote deficit is mainly due to sub-structure, and ii) strong gene flow among populations, leading to low F_{ST} and to no clear genetic structure at the explored spatial scale. Soil transport through both agricultural machinery and the transport of leek seedlings is probably responsible of the very strong *H. carotae* migration among fields and among production areas. Measures should be considered to limit the passive spread of *H. carotae*.

Introduction

Plant-parasitic nematodes are distributed worldwide and pose a major threat for numerous crops of high agricultural interest. They are obligatory parasites and feed only on their host plants leading to poor plant growth and severe crop losses (Nicol *et al.*, 2011). In Europe, the ban of the chemical nematicide 1,3 dichloropropene (CE 2076/2002), which was used thanks to dispensations (CE 1107/2009) until 2018 in France, gives a strong opportunity to the use of new control solutions, such as plant resistances and biocontrol products. However, these new control methods may be more dependent on the evolutionary potential of nematode population (i.e. the ability for a population to adapt and evolve in its environment), which mainly depends on gene flow among populations (McDonald & Linde, 2002). In cyst nematode species, population genetic structure are mainly the result of the active dispersal of free-living stages in the soil (i.e. second-stage juveniles and males) at short distances, leading to strong heterozygote deficits (e.g. Montarry *et al.*, 2015), and of the passive dispersal of cysts at long distances. Indeed, massive gene flow were revealed for the potato cyst nematode *Globodera pallida* (Picard *et al.*, 2004), the beet cyst nematode *Heterodera schachtii* (Plantard & Porte, 2004) and the tobacco cyst nematode *G. tabacum* (Alenda *et al.*, 2014). The migration of cysts was subsequent to commercial trades at large geographical scales, resulting in a strong geographical structure (Plantard *et al.*, 2008; Boucher *et al.*, 2013; Alenda *et al.*, 2014) and also to agricultural activities resulting in a lack of structure at finer geographical scales (e.g. Alenda *et al.*, 2014). As a new recent example, the study of the genetic structure of seventeen European populations of the carrot cyst nematode *Heterodera carotae* revealed that i) *H. carotae* populations were characterised by a strong heterozygote deficit, ii) they were grouped into two genetic clusters geographically structured and iii) gene flow were low among populations in each cluster (Gautier *et al.*, 2019). However, there is a lack of knowledge of the genetic structure of the populations of this nematode at a more restricted spatial scale.

Heterodera carotae had a very narrow host range constituted of different subspecies of *Daucus carota* L. and a wild Apiaceae, *Torilis leptophylla* L. (Mugniery & Bossis, 1988). It is a polyvoltine species able to perform up to four generations during a growing season in favourable conditions (Subbotin *et al.*, 2010). As a result, infestations in the field correspond to irregular areas of stunted plants, characterised by small, abnormally developed and unmarketable carrots. *Heterodera carotae* is present in most of carrot-growing regions worldwide: in the state of Michigan in the USA (Berney & Bird, 1992), in the province of Ontario in Canada (Yu *et al.*, 2017), in an important Mexican carrot producing area (Escobar-Avila *et al.*, 2018), in sixteen countries of Europe including France (Osborne, 1971; Mugniéry & Bossis 1988; Gautier *et al.*, 2019) and in South-Africa (Subbotin *et al.*, 2010). Ranges of estimated carrot crop-losses related to *H. carotae* were estimated from 20 to 90% in Italy (Greco *et al.*, 1993) and more than 35% in Ontario (Yu *et al.*, 2017).

Till now, the French carrot production system relied on the dispensations granted for the chemical nematicide 1,3 dichloropropene. The development of alternative means of management of *H. carotae*, economically and environmentally safe, is thus essential in carrot-growing regions. Since 10 years, several alternatives to current chemical nematicides have been explored: soil solarisation, biofumigation, biological control and plant genetic resistance (e.g. Grevsen, 2012; D'Addabbo *et al.*, 2013). Whatever the alternative control measure, the knowledge of the adaptive abilities of *H. carotae* populations constitutes a key factor in the development of sustainable strategies, i.e. strategies that reduce the probability of adaptive events.

The first goal of the present study was thus to investigate the genetic diversity and structure of *H. carotae* populations using microsatellite genotyping of individuals collected within Lower Normandy, the major carrot producing region infested by *H. carotae* in France, which includes three distinct production areas: Créances, Val-de-Saire and Mont St-Michel.

The second goal was to estimate the relative contribution of inbreeding and Wahlund effect to the heterozygote deficit highlighted in this polyvoltine species (Gautier *et al.*, 2019), using *H. carotae* populations sampled at the plant scale.

Materials and methods

Sampling of nematode cysts

Cysts of the carrot cyst nematode, *Heterodera carotae*, were collected in December 2016 from commercial carrot fields, all located in Lower Normandy, one of the two major French regions producing carrots. In contrast with Aquitaine (the second major French region producing carrots), the extensive occurrence of *H. carotae* in Lower Normandy lead to important yield losses. Three distinct production areas were investigated in Lower Normandy: Créances, Val-de-Saire and Mont St-Michel. A sampling strategy was conducted in order to study two types of populations: populations collected at the field scale and populations collected at the plant scale. The GPS coordinates of each field were recorded (Table 1).

Twenty-two populations were collected at the field spatial scale: two fields in the Mont St-Michel area, five fields in the Val-de-Saire area and 15 in the Créances area. According to Garcia *et al.* (2018), ten sample points were defined alongside the longest diagonal of each field. The ten points (depth of 15 cm using a manual auger (diam. 2.5 cm)) were pooled, resulting in one sample per field. Geographical distances between the three production areas varied between 65-74 km (from Mont St-Michel to Créances) to 120 km (from Mont St-Michel to Val-de-Saire) and fields in each area were separated from each other by 0.1 to 14 km.

For the investigations at the plant scale, soil samples were collected around roots of individual carrot plants *Daucus carota* subsp. *sativus* alongside the diagonal of two fields located in the Créances area, named Cre4 and Den3. Nine and 10 distinct *H. carotae* populations

were collected from distinct plants in Cre4 and Den3, respectively. Within each field, sampled populations were separated from each other by 10 m.

Nematode cysts were extracted from 100 g of soil by a Kort elutriator. The number of cysts in 100 g of soil ranged from 15 to 280 and the estimated number of second-stage juveniles per gram of soil ranged from 3.4 to 64.3. To obtain at least 40 cysts per population, up to 500 g of soil were extracted for some populations.

Microsatellite genotyping

In order to assess the genetic diversity of the carrot cyst nematode populations, we used a set of 13 microsatellite markers developed by Gautier *et al.* (2019). For each population, 40 second-stage juveniles (J2) from 40 distinct cysts, randomly chosen, were genotyped. DNA extractions were performed as described in Gautier *et al.* (2019). DNAs were diluted with a 1:2 dilution ratio, and 2 µL was used for the microsatellite genotyping. PCR multiplex was performed in 5 µL of working volume, containing 1X of Type-it Microsatellite PCR kit (Qiagen) and 0.2 µM of each primer. Cycling conditions are the same as those described by Gautier *et al.* (2019), i.e. an initial denaturation at 95 °C for 5 min, followed by 30 cycles of denaturation at 95 °C for 30 s, annealing at 57 °C for 90 s and extension at 72 °C for 30 s, followed by a final extension at 60 °C for 30 min. PCR products were then diluted to 1:40 in sterile water, and 3 µL of this dilution was mixed with 0.05 µL of GeneScan 500 LIZ Size Standard (Applied Biosystems) and 5 µL of formamide (Applied Biosystems). Analyses of PCR products were conducted on an ABI Prism®3130xl sequencer (Applied Biosystems). Allele sizes were identified using the automatic calling and binning procedure of GeneMapper v4.1 (Applied Biosystems) and completed by a manual examination of irregular results.

Dataset cleaning

Among the 13 microsatellite loci (Hc07, Hc29, Hc35, Hc40, Hc49, Hc55, Hc59, Hc63, Hc72, Hc76, Hc87, Hc91 and Hc94), 12 markers were retained. Hc91 was discarded because the amplification of this locus failed for 55 % of our individuals. This marker was also the one showing the highest frequency of potential null alleles (i.e. 28.7%) in the study of Gautier *et al.* (2019), which comforted us in the decision to remove it. For each collected population, 33 to 40 J2 from distinct cysts were successfully genotyped.

A preliminary factorial correspondence analysis (FCA) was performed using GENETIX 4.05.2 (Belkhir *et al.*, 2004) on all individuals from the cysts collected at the field scale (i.e. 822 individuals) and showed that all individuals were closely grouped, except for 114 individuals from four populations from the Val-de-Saire area (all individuals from populations VDS3 and VDS6, 33/39 individuals from SIL1 and 11/33 individuals from VDS4) which were grouped separately. The high genetic distance between the two groups suggested the presence of the cabbage cyst nematode *Heterodera cruciferae* which resembles *H. carotae*. In order to check the possible membership of those 114 individuals to the *H. cruciferae* species, 32 J2 from 32 distinct cysts of two *H. cruciferae* populations, maintained in our lab collection (and multiplied on cauliflower), were genotyped and included to the dataset before rerunning the FCA. Moreover, to confirm the membership of our populations to the *H. carotae* species, two reference *H. carotae* populations (i.e. 36 individuals) from Gautier *et al.* (2019), both multiplied on carrot, were added to this analysis. The FCA revealed two groups: the 114 J2 were clearly grouped with all *H. cruciferae* individuals from the reference populations and all the other individuals were clearly grouped with the reference *H. carotae* populations (Fig. S1, Supporting information). Consequently, the *H. cruciferae* individuals were excluded from the final dataset as well as the six *H. carotae* remaining individuals of the population SIL1, insufficient to constitute a population.

We finally analysed 19 *H. carotae* populations (i.e. two from the Mont St-Michel area, two from the Val-de-Saire area and 15 from the Créances area) at the field scale (i.e. 702 individuals) and 19 *H. carotae* populations (i.e. 768 individuals) at the plant scale, which were genotyped using a set of 12 polymorphic microsatellite markers.

Data analysis

Analyses at the field scale

Genotypic linkage disequilibrium among all pairs of loci was assessed using a Markov Chain approximation of the Fisher's exact test, as implemented in GENEPOP 4.0.7 (Raymond & Rousset, 1995). A Bonferroni adjustement was applied to take into account multiple testing, i.e. $\alpha = 0.05$ was lowered to $\alpha = 0.00076$ for 66 comparisons.

Null allele frequencies were estimated for each locus across all populations using the likelihood-based method of Chybicki & Burczyk (2009) implemented in the INEst program. Moreover, the relationship between the percentage of missing data for each locus and F_{IS} was examined (Beaumont *et al.*, 2001) with the Spearman's rank correlation coefficient rho using the statistical software R version 3.6.1. A positive relationship between F_{IS} and missing data would indicate that amplification failure is due to individuals bearing a null allele at the homozygous state.

Allelic richness (Ar) was estimated using the rarefaction method implemented in POPULATIONS 1.2.32 (Langella, 1999), which estimated the mean number of alleles per locus for a reduced sample size. An unbiased estimate of gene diversity (H_{nb} according to Nei (1978)) and deviation from random mating (F_{IS}) were computed using GENETIX 4.05.2 (Belkhir *et al.*, 2004). The statistical significances of F_{IS} were estimated using the allelic permutation method (10,000 permutations) implemented in GENETIX.

To explore the genetic structure of the 19 *H. carotae* populations at the regional spatial scale, the Bayesian clustering algorithms implemented in STRUCTURE 2.3.4 (Pritchard *et al.*, 2000) was run on a reduced dataset free of any missing data (i.e. 595 individuals). According to Gautier *et al.* (2019), which followed the recommendations of Wang (2017), default priors were chosen except for alpha, for which the value was set to 0.0526 (i.e. 1 / p, p being the number of populations) and the uncorrelated allele frequency model was used. The initial burn-in period consisted of 1,000,000 iterations and the number of Markov chain Monte Carlo (MCMC) repetitions was 3,000,000. The K value was set from 1 to 20 (i.e. p + 1) and thirty different runs were executed for each K. We applied Structure Harvester Web ver.0.6.94 (Earl & vonHoldt, 2012) to determine the most likely number of clusters statistically determined using the ad-hoc Evanno statistic ΔK (Evanno *et al.*, 2005).

The hierarchical structuring was assessed with an AMOVA model using ARLEQUIN v.3.5 (Excoffier & Lischer, 2010) and considering three hierarchical levels: among production areas (Créances, Val-de-Saire and Mont St-Michel), among populations within each production area and within populations.

The differentiation coefficients between each pair of populations (F_{ST}) were computed using GENEPOP 4.5.1 according to Weir & Cockerham (1984), and their statistical significances were estimated by 5,000 random permutations of individuals among populations. A Bonferroni adjustement was applied to take into account multiple testing, i.e. $\alpha = 0.05$ was lowered to $\alpha = 0.00029$ for 171 comparisons. A pattern of isolation by distance (IBD) was tested by calculating the correlation between the matrices of pairwise genetic distances (F_{ST} / (1 - F_{ST})) and the natural logarithm of geographic distance for each pair of populations (Rousset, 1997). The statistical significance of the correlation was assessed through a Mantel test (10,000 permutations) using XLSTAT 2019.3.1 (Addinsoft SARL).

Analyses at the plant scale

The unbiased estimate of gene diversity (H_{nb}) and the F_{IS} were computed for each of the 19 *H. carotae* populations collected at the plant scale as described above. The statistical significance of F_{IS} values for each population was tested using the allelic permutation method (10,000 permutations) implemented in GENETIX.

Because heterozygote deficits in cyst nematodes could be due to a Wahlund effect (i.e. sub-structure) and/or to consanguinity (Montarry *et al.*, 2015), we used the method of Overall & Nichols (2001) in order to calculate a likelihood surface for the genetic correlation due to population subdivision (θ) and the proportion of the population practicing consanguinity (C). The method, which is based on the argument that consanguinity and sub-structure generate distinctive patterns of homozygosity in multilocus data, was applied assuming a degree of relatedness of 1/4 (see Montarry *et al.*, 2015) to all *H. carotae* populations showing significant heterozygote deficits. Likelihood estimates where obtained by searching for the maximum of the likelihood function over a grid of 10,000 combinations of θ and C values. Moreover, graphs of the likelihood surface were obtained for each nematode population using the statistical software R version 3.6.1.

Results

Genetic features of *H. carotae* field populations

At the fields scale, using our set of 12 microsatellites, we identified 54 alleles among the 19 *H. carotae* populations (i.e. 702 individuals) genotyped, with two (for Hca-07) to 10 (for Hca-63) alleles per locus. Using the Bonferroni's adjustment no significant linkage disequilibrium was detected among the 66 pairs of loci.

The percentage of null allele estimated by INEst averaged 6.23% among our 12 microsatellite markers. The percentage of potential null allele ranged from 0% (locus Hca-29)

to 15% (locus Hca-63) and there was no significant correlation between the percentage of missing data and F_{IS} (rho = 0.253; P = 0.297). Consequently, we assumed that null alleles would have no strong effect on the population genetics analyses performed hereafter.

The genetic diversity was quite similar among the different *H. carotae* populations: the allelic richness (Ar), estimated on a reduced sample of 16 individuals, ranged from 2.28 to 2.77 alleles per locus and the unbiased expected heterozygoty (H_{nb}) ranged from 0.30 to 0.45 (Table 1). Among the 19 populations, only four populations were at the Hardy-Weinberg equilibrium (F_{IS} not significantly different to zero). All the 15 remaining populations showed strong heterozygote deficits (F_{IS} ranging from 0.088 to 0.198 - Table 1).

Genetic structure among *H. carotae* field populations

Although the Bayesian clustering analysis identified K = 3 as the optimal number of genetic clusters, there was no clear genetic structure. Indeed, only a small proportion of individuals were well assigned to one or the other clusters: only 10.6% of individuals were assigned to a cluster with a percentage of assignation higher than 95% (6.9% to cluster 1, 1.7% to cluster 2 and 2.0% to cluster 3). Moreover, the three clusters were represented in each of the 19 populations (Fig. 1), even if Bre1 was mainly assigned to cluster 1, StM4 and Sil5 were mainly assigned to cluster 2 and Den3 was mainly assigned to cluster 3 (the average percentages of assignation of those populations to the corresponding clusters being 75.1%, 72.4%, 65.7% and 60.2%, respectively). Anyway, the three genetic clusters did not correspond to the three production areas (Fig. 1).

The AMOVA performed on *H. carotae* populations partitioned according to the three carrot production areas revealed that only 3.24% of the genetic diversity was explained by the productions areas and only 3.93% by the populations within each production area, while the diversity within populations explained 92.83% of the total variation.

256

257 **Genetic differentiation between *H. carotae* populations**

258 At the field scale, F_{ST} values were low, ranging from 0 to 0.18 (Fig. 2). Among the 171 pairwise
259 comparisons, only 96 were significant after Bonferroni adjustement. The lowest pairwise F_{ST}
260 values were observed between populations from the Créances production area, except for the
261 population Bre1 (Fig. 2). Bre1 displayed the highest F_{ST} values observed (from 0.05 to 0.18),
262 significant for all of the pairwise comparisons, indicating some degree of differentiation
263 between Bre1 and all other populations. High F_{ST} values were also observed for populations
264 Sil5 and StM3 from Val-de-Saire and Mont-St-Michel, respectively, while VDS4 and StM4,
265 collected also from those production areas, showed low F_{ST} values in most comparisons (Fig.
266 2). Altogether, this suggests that important gene flow occured, even between the different
267 production areas in Lower Normandy.

268 Moreover, the positive correlation between genetic and geographic distances (Fig. 3)
269 highlighted an IBD pattern, showing that gene flow occurred among *H. carotae* populations
270 and that their intensity was higher between the closest fields.

271

272 **The heterozygote deficit in *H. carotae* populations**

273 Among the 19 *H. carotae* populations sampled at the plant scale, 12 showed a significant
274 heterozygote deficit, eight in the field Cre4 and four in the field Den3, the remaining
275 populations being at the Hardy-Weinberg equilibrium (Table 2).

276 Among those 12 populations, the heterozygote deficit was attributed only to
277 consanguineous mating for Cre4.1 and Cre4.7 populations (Table 2 and Fig. S2 supporting
278 information). For all other populations, the most likely parameter combination for explaining
279 the heterozygote deficit included a high level of sub-structure (a Wahlund effect), and there was

even no evidence of consanguinity for three populations, Cre4.3, Cre4.4 and Den3.3 (Table 2 and Fig. S2 supporting information).

Discussion

The goal of this study was to describe the genetic structure of *H. carotae* populations at a spatial scale corresponding to the main infested French carrot-producing region, i.e. Lower Normandy, and to disentangle the causes of the heterozygote deficit in this polyvoltine species. Through the microsatellite genotyping of populations collected at the plant and at the field scales, we showed i) that the heterozygote deficit is mainly due to sub-structure, and ii) strong gene flow among populations, leading to low F_{ST} and to no clear genetic structure at the explored spatial scale.

To determine the extent of *H. carotae* distribution and to better control this nematode in carrot-producing regions, the accurate detection and identification of the carrot cyst nematode is a fundamental prerequisite. *H. carotae* belongs to the *Goettingiana* group which includes *H. goettingiana, H. carotae, H. urticae,* and *H. cruciferae* (Subbotin *et al.*, 2010). *H. carotae* is morphologically and genetically very close to the cabbage cyst nematode, *H. cruciferae* and the correct diagnosis is difficult and time consuming. rRNA and mitochondrial molecular markers such as ITS, cytochrome c oxidase 1 subunit (coxI) region (Vovlas *et al.*, 2017, Escobar-Avila *et al.*, 2018) and coxI derived primers set (Madani *et al.*, 2018) can help in the identification of members of the *Goettingiana* group, but none are able to provide an unequivocal distinction between *H. carotae* and *H. cruciferae*. As a result, only a host range test using carrot allowed to accurately distinguish these two species (Escobar Avila *et al.*, 2018). The microsatellite markers used in the present study successfully amplified both *H. carotae* and *H. cruciferae,* and the high degree of genetic differentiation observed between reference *H. carotae* populations

and reference *H. cruciferae* populations allowed us to well distinguish *H. carotae* and *H. cruciferae* individuals in our dataset. Due to the conservation of microsatellite loci among taxa, the set of microsatellite markers initially developed for *H. carotae* (Gautier *et al.*, 2019) could be used i) to explore the genetic diversity of *H. cruciferae*, but also ii) to develop a diagnostic tool able to differentiate *H. carotae* from *H. cruciferae.* Indeed, combined into a single real-time PCR assay, diagnostic markers for three cyst nematode species, *G. pallida*, *G. rostochiensis* and *H. schachtii*, were identified and developed from microsatellite loci (Gamel *et al.*, 2017). We thus propose to investigate *H. carotae* microsatellite loci, including the large number of discarded loci (monomorphic loci or loci that contain few repeats of the microsatellite motif), to develop a molecular tool for the diagnosis of *H. carotae* and *H. cruciferae*.

If an accurate diagnosis is the first step in selecting appropriate control measures, a fine knowledge of the active and passive dispersal capabilities of the nematode is essential to promote the best and sustainable management strategies. Our results showed that 15/19 *H. carotae* populations sampled at the field scale and 12/19 populations sampled at the plant scale deviate from the Hardy-Weinberg equilibrium and show significant positive F_{IS} values. Such heterozygote deficit was previously highlighted for several cyst nematode species at the field scale (for *Globodera pallida* – Picard *et al.*, 2004, *Heterodera schachtii* – Plantard & Porte, 2004, *G. tabacum* – Alenda *et al.*, 2014, *H. glycines* – Wang *et al.*, 2015, *H. avenae* – Wang *et al.*, 2018 and *H. carotae* – Gautier *et al.*, 2019) and at the plant scale (for *G. pallida*, *G. tabacum* and *H. schachtii* - Montarry *et al.*, 2015). As for *G. tabacum* and *H. schachtii*, which performed also several generations per growing season, the heterozygote deficit of *H. carotae* populations was mainly attributed to substructure (Wahlund effect) at the spatial scale of the carrot's rhizosphere. The fact that footprints of consanguineous mating were also detected supports the hypothesis that from an isolated cyst, the restricted active dispersal capabilities of second-stage

juveniles lead in a first time to consanguineous mating and then to the differentiation of sub-populations during the next generations (Montarry *et al.*, 2015).

The analysis of partitioning of molecular variability (AMOVA) showed that a very small part of the genetic variability was observed among the three carrot production areas (Créances, Val-de-Saire and Mont St-Michel) and among populations within each production area. This result combined with the absence of genetic structure within Lower Normandy revealed the occurrence of strong gene flow among *H. carotae* populations. While *H. carotae* juveniles exhibit limited active dispersion capabilities in the soil, dormant eggs are able to disperse over long distances within the cysts through natural means and human activities. In the present case, we can for instance easily imagine that sea winds can lift up both sandy soil and cysts. However, human activities and the resulting soil movements play most certainly an important role in the *H. carotae* dispersion. Extensive gene flow among populations were also highlighted at comparable spatial scales for other cyst nematodes, such as the pale potato cyst nematode (e.g. Picard *et al.*, 2004) and the beet cyst nematode (Plantard & Porte, 2004). It is most probable that such extensive gene flow occur thanks to soil transport through agricultural machinery, especially during the harvest process, and to the exchange of plant material (Goeminne *et al.*, 2015). During a carrot-growing season, only few cultural practices lead to soil transports. Cysts can be transported from fields to fields in the soil stuck on farm implement, but there is no exchange of carrot plants (and soil) as in the case of seed potato tubers. However, fields in Lower Normandy are cultivated with leeks and carrots and unlike the carrot that is sown directly, the young leek plants (two months old) are traditionally transplanted into the field. Thus, passive spread of *H. carotae* by the transport of infected soil bound to leek seedlings is probably responsible of the extensive gene flow observed among production areas, and soil transport thought both agricultural machinery and the transport of

353 leek seedlings are probably responsible of the very strong *H. carotae* migration among fields
354 within each production area.

355 Considering the geographical localization of each field, a significant isolation by
356 distance pattern was highlighted, showing that the intensity of gene flow was higher among
357 close fields than among distant fields. This pattern is congruent with the different means of soil
358 transport identified, i.e. agricultural machinery and leek seedlings within a production area and
359 only leek seedlings among the different production areas. Moreover, the variability in the
360 intensities of gene flow is true at the scale of the Lower Normandy, with F_{ST} higher between
361 fields of different production areas than between fields of the same production area, but also at
362 a finer spatial scale. Indeed, within the Créances production area, F_{ST} values observed between
363 the Bre1 population and the others ones were the highest of the F_{ST} matrix. In this production
364 area, all *H. carotae* populations were collected in infested fields located around the Créances
365 town or along the main south-north road, while Bre1 was sampled in a more isolated field,
366 located near the sea (about 1 km from the road).

367 In lower Normandy, the lack of strong genetic structure and thus the genetic
368 homogeneity observed in *H. carotae* populations are both factors suggesting that the use of
369 control means based on plant resistance may be efficient in all fields. Conversely, the strong
370 gene flow highlighted among fields and among the three studied areas show that any adaptive
371 events, even in a single field, is associated with a very high risk of spreading. As a result,
372 measures should be considered to limit the passive spread of *H. carotae*: and therefore further
373 investigations are required to identify the main dissemination vectors used by *H. carotae*. In
374 the current context, i.e. the recent total withdrawal of 1,3 dichloropropene which lets growers
375 without effective method to control *H. carotae* in Lower Normandy, growers will be tempted
376 to exploit nematode-free fields in the coming years. But, without strong prophylactic measures,
377 the risk to see these fields becoming also quickly infested remains high.

Acknowledgments We gratefully acknowledge the SILEBAN for their help in the sampling of *Heterodera carotae* populations and for useful discussions about the transport of leek seedlings. Camille Gautier is supported by PhD grant from Groupe Roullier and ANRT (Association Nationale Recherche Technologie).

References

Alenda C, Montarry J, Grenier E, 2014. Human influence on the dispersal and genetic structure of French *Globodera tabacum* populations. *Infection, Genetics and Evolution* **27**, 309-17.

Beaumont M, Barratt EM, Gottelli D *et al.*, 2001. Genetic diversity and introgression in the Scottish wildcat. *Molecular Ecology* **10**, 319-36.

Belkhir K, Borsa P, Chikhi L, Raufaste N, Bonhomme F, 2004. GENETIX 4.05, logiciel sous Windows TM pour la génétique des populations. Laboratoire Génome, Populations, Interactions, CNRS UMR 5000, Université de Montpellier II, Montpellier (France).

Berney M, Bird G, 1992. Distribution of *Heterodera carotae* and *Meloidogyne hapla* in Michigan carrot production. *Journal of Nematology* **24**, 776-8.

Boucher AC, Mimee B, Montarry J *et al.*, 2013. Genetic diversity of the golden potato cyst nematode *Globodera rostochiensis* and determination of the origin of populations in Quebec, Canada. *Molecular Phylogenetics and Evolution* **69**, 75-82.

Chybicki IJ, Burczyk J, 2009. Simultaneous estimation of null alleles and inbreeding coefficients. *Journal of Heredity* **100**, 106-13.

D'Addabbo T, Carbonara T, Argentieri MP *et al.*, 2013. Nematicidal potential of *Artemisia annua* and its main metabolites. *European Journal of Plant Pathology* **137**, 295-304.

Earl DA, vonHoldt BM, 2012. STRUCTURE HARVESTER: a website and program for visualizing STRUCTURE output and implementing the Evanno method. *Conservation Genetics Resources* **4**, 359-61.

Escobar-Avila IM, Óliver E, Subbotin SA, Tovar-Soto A, 2018. First report of carrot cyst nematode *Heterodera carotae* in Mexico: morphological, molecular characterization and host range study. *Journal of Nematology* **50**, 229-42.

Evanno G, Regnaut S, Goudet J, 2005. Detecting the number of clusters of individuals using the software STRUCTURE: a simulation study. *Molecular Ecology* **14**, 2611-20.

409 Excoffier L, Lischer HEL, 2010. Arlequin suite ver 3.5: a new series of programs to perform
410 population genetics analyses under Linux and Windows. *Molecular Ecology Resources*
411 **10**, 564-7.
412 Gamel S, Letort A, Fouville D, Folcher L, Grenier E, 2017. Development and validation of real-
413 time PCR assays based on novel molecular markers for the simultaneous detection and
414 identification of *Globodera pallida*, *G. rostochiensis* and *Heterodera schachtii*.
415 *Nematology* **19**, 789-804.
416 Garcia N, Folcher L, Biju-Duval L, Maupetit A, Ricci B, Grenier E, 2018. Impact of agricultural
417 practices and environmental variables on plant-parasitic nematode communities in fields
418 at a landscape scale. *Nematology* **20**, 211-33.
419 Gautier C, Esquibet M, Fournet S *et al.*, 2019. Microsatellite markers reveal two genetic groups
420 in European populations of the carrot cyst nematode *Heterodera carotae*. *Infection,*
421 *Genetics and Evolution* **73**, 81-92.
422 Goeminne M, Demeulemeester K, Lanterbecq D, De Proft M, Viaene N, 2015. Detection of
423 field infestations of potato cyst nematodes (PCN) by sampling soil from harvested
424 potatoes. *Aspect of Applied Biology* **130**: 105-10.
425 Greco N, D'Addabbo T, Brandonisio A, Elia F, 1993. Damage to Italian crops caused by cyst-
426 forming nematodes. *Journal of Nematology* **25**: 836-42.
427 Grevsen K, 2012. Biofumigation with *Brassica juncea* pellets and leek material in carrot crop
428 rotations. *Acta Horticulturae* **933**, 427-31.
429 Langella O, 1999. Populations 1.2.31. Population Genetic Software (Individuals or Populations
430 Distances, Phylogenetic Trees) 2012. [http://bioinformatics.org/~tryphon/populations/].
431 Madani M, Palomares-Rius JE, Vovlas N, Castillo P, Tenuta M, 2018. Integrative diagnosis of
432 carrot cyst nematode (*Heterodera carotae*) using morphology and several molecular

markers for an accurate identification. *European Journal of Plant Pathology* **150**, 1023-39.

McDonald BA, Linde C, 2002. Pathogen population genetics, evolutionary potential, and durable resistance. *Annual Review of Phytopathology* **40**, 349-79.

Montarry J, Jan PL, Gracianne C *et al.*, 2015. Heterozygote deficits in cyst plant-parasitic nematodes: possible causes and consequences. *Molecular Ecology* **24**, 1654-67.

Mugniery D, Bossis M, 1988. *Heterodera carotae* Jones, 1950 - Gamme d'hôtes, vitesse de développement, cycle. *Revue de Nématologie* **11**, 307-13.

Nei, M, 1978. Estimation of average heterozygosity and genetic distance from a small number of individuals. *Genetics* **89**, 583-590.

Nicol JM, Turner SJ, Coyne D, Den Nijs L, Hockland S, Maafi ZT, 2011. Current nematode threats to world agriculture. In: Jones J, Gheysen G, Fenoll C, eds. *Genomics and Molecular Genetics of Plant-Nematode Interactions*. Dordrecht, The Netherlands: Springer Science+Business Media BV, 21-43.

Osborne P, 1971. First record of *Heterodera catotae* in Scotland. *Plant Pathology* **20**, 148.

Overall ADJ, Nichols RA, 2001. A method for distinguishing consanguinity and population substructure using multilocus genotype data. *Molecular Biology and Evolution* **18**, 2048-56.

Picard D, Plantard O, Scurrah M, Mugniery D, 2004. Inbreeding and population structure of the potato cyst nematode (*Globodera pallida*) in its native area (Peru). *Molecular Ecology* **13**, 2899-908.

Plantard O, Picard D, Valette S, Scurrah M, Grenier E, Mugniéry D, 2008. Origin and genetic diversity of Western European populations of the potato cyst nematode (*Globodera pallida*) inferred from mitochondrial sequences and microsatellite loci. *Molecular Ecology* **17**, 2208–18.

458 Plantard O, Porte C, 2004. Population genetic structure of the sugar beet cyst nematode
459 *Heterodera schachtii*: a gonochoristic and amphimictic species with highly inbred but
460 weakly differentiated populations. *Molecular Ecology* **13**, 33-41.
461 Pritchard JK, Stephens M, Donnelly P, 2000. Inference of population structure using multilocus
462 genotype data. *Genetics* **155**, 945-59.
463 Raymond M, Rousset F, 1995. Genepop Version1.2: population genetics software for exact
464 tests and ecumenicism. *Journal of Heredity* **86**, 248–9.
465 Rousset F, 1997. Genetic differentiation and estimation of gene flow from F-statistics under
466 isolation by distance. *Genetics* **145**, 1219-28.
467 Subbotin SA, Mundo-Ocampo M, Baldwin JG, 2010. *Systematics of Cyst Nematodes*
468 *(Nematodes: Heteroderinae), Volume 8, Part B*. Leiden, The Netherlands: Brill.
469 Vovlas A, Santoro S, Radicci V, Leonetti P, Castillo P, Palomares-Rius JE, 2017. Host-
470 suitability of black medick (*Medicago lupulina* L.) and additional molecular markers for
471 identification of the pea cyst nematode *Heterodera goettingiana*. *European Journal of*
472 *Plant Pathology* **149**, 193-9.
473 Wang HM, Zhao HH, Chu D, 2015. Genetic structure analysis of populations of the soybean
474 cyst nematode, *Heterodera glycines*, from north China. *Nematology* **17**, 591-600.
475 Wang J, 2017. The computer program structure for assigning individuals to populations: easy
476 to use but easier to misuse. *Molecular Ecology Resources* **17**, 981-90.
477 Wang X, Ma J, Liu H, Liu R, Li H, 2018. Development and characterization of EST-derived
478 SSR markers in the cereal cyst nematode *Heterodera avenae*. *European Journal of Plant*
479 *Pathology* **150**, 105-13.
480 Weir BS, Cockerham CC, 1984. Estimating F-statistics for the analysis of population structure.
481 *Evolution* **38**, 1358-70.

Yu Q, Ponomareva E, Van Dyk D *et al.*, 2017. First report of the carrot cyst nematode (*Heterodera carotae*) from carrot fields in Ontario, Canada. *Plant Disease* **101**, 1056.

Data Availability

Two files containing the genotypic data (Genepop format) for the different *Heterodera carotae* populations sampled at the plant scale (H_carotae_plants.txt) and at the field scale (H_carotae_fields.txt) are available at data.inra.fr (https://doi.org/10.15454/MLMDVE).

Supporting Information legends

Fig. S1 Factorial correspondence analysis (FCA) performed on the 822 individuals collected at the field scale (circles). The 114 individuals which formed a distinct group (black circles) from all the other individuals (grey circles), were clearly grouped with the 64 *H. cruciferae* individuals coming from two reference populations (white triangles). All the other individuals were clearly grouped with the 36 individuals from the two reference *H. carotae* populations (white squares). The two first axes explained 22% and 3.5% of the genetic variability, respectively.

Fig. S2 Likelihood surfaces showing estimated θ and C values with 95 and 99% confidence envelopes for the 12 *H. carotae* populations sampled at the spatial scale of the plant showing significant heterozygote deficits (eight populations from the field Cre4 and four populations from the field Den3).

Figure legends

Fig. 1 Bayesian clustering analysis (STRUCTURE) of the 595 *H. carotae* individuals (i.e. the dataset free of any missing data) coming from the 19 populations sampled at the field scale. Assignment probabilities of individuals are presented for K = 3. On the graph at the bottom, each vertical line represents an individual for which the genetic assignment is partitioned into three clusters, represented by three colors, and vertical white dotted lines separate each of the 19 populations. The map at the top shows the geographical location of the 19 *H. carotae* populations and their membership proportion of clusters. In the production area of Créances, the dot line represents the main south-north road.

Fig. 2 Matrix of pairwise F_{ST} between the 19 *H. carotae* populations sampled at the field scale. ns indicates non-significant differentiation between two populations. Populations were horizontally separated according to the three carrot production areas: Créances, Val-de-Saire and Mont St-Michel.

Fig. 3 Isolation by distance pattern between genetic differentiation, measured as $F_{ST} / (1 - F_{ST})$, and geographic distance (natural logarithm of the distance in m) for pairwise *H. carotae* populations.

527 **Table 1** *Heterodera carotae* populations collected at the field scale in three carrot production
528 areas in Lower Normandy. For each of the 19 populations, the table shows the production area,
529 the district, the GPS coordinates of each field, the number of successfully genotyped individuals
530 (N), the genetic diversity indices (H_{nb} and Ar) and the departure from Hardy-Weinberg
531 equilibrium (F_{IS}). F_{IS} values significantly different to zero are indicated by a star.

532

Population	**Production area**	**District**	**GPS coordinates**		**N**	**H_{nb}**	**Ar (n=16)**	**F_{IS}**
Bre1	Créances	Bretteville / Ay	49°15'01.90"N	1°39'02.83"O	33	0,447	2,56	0,185*
Bre2c	Créances	Bretteville / Ay	49°15'46.95"N	1°38'34.74"O	36	0,372	2,52	0,198*
Bre2p	Créances	Bretteville / Ay	49°15'46.95"N	1°38'34.74"O	36	0,389	2,43	0,139*
Cre1	Créances	Créances	49°12'10.52"N	1°34'56.90"O	37	0,332	2,42	0,037
Cre2	Créances	Créances	49°12'13.78"N	1°34'57.51"O	40	0,380	2,52	0,103*
Cre3	Créances	Créances	49°12'27.59"N	1°34'46.36"O	39	0,366	2,45	0,154*
Cre4	Créances	Créances	49°12'44.06"N	1°34'37.87"O	40	0,295	2,30	0,090*
Cre5	Créances	Créances	49°12'36.14"N	1°34'46.58"O	40	0,343	2,32	0,088*
Cre6	Créances	Créances	49°12'09.51"N	1°35'03.02"O	39	0,373	2,35	0,142*
Cre7	Créances	Créances	49°12'42.03"N	1°35'42.04"O	39	0,356	2,47	-0,041
Cre8	Créances	Créances	49°12'31.48"N	1°34'31.51"O	38	0,336	2,33	0,046
StG1	Créances	Saint Germain / Ay	49°14'33.88"N	1°37'35.42"O	39	0,336	2,36	0,166*
StG2	Créances	Saint Germain / Ay	49°14'23.13"N	1°37'27.58"O	34	0,386	2,54	0,135*
Den2	Créances	Denneville	49°18'34.75"N	1°40'51.46"O	34	0,381	2,28	0,062
Den3	Créances	Denneville	49°18'46.96"N	1°40'51.86"O	40	0,333	2,43	0,133*
SIL5	Val-de-Saire	Gatteville-le-Phare	49°40'9.90"N	1°16'37.57"O	36	0,427	2,52	0,094*
VDS4	Val-de-Saire	Montfarville	49°39'26.73"N	1°14'53.35"O	22	0,437	2,75	0,118*
StM3	Mont S^{t}-Michel	Le Mont Saint-Michel	48°36'56.20"N	1°31'47.51"O	40	0,346	2,35	0,195*
StM4	Mont S^{t}-Michel	Beauvoir	48°36'19.85"N	1°31'51.02"O	40	0,438	2,77	0,119*

533

534 **Table 2** *Heterodera carotae* populations collected at the plant scale in two carrot fields (Cre4
535 and Den3). For each of the 19 populations, the table shows the number of genotyped individuals
536 (N), the genetic diversity index (H_{nb}), the F_{IS} values and their significance (values significantly
537 different to zero are indicated by a star) and θ and C values, corresponding to the maximum-
538 likelihood, for each population showing a significant heterozygote deficit.
539

Population	**N**	**H_{nb}**	**F_{IS}**	**θ**	**C**
Cre4-1	40	0.30	0.132*	0.00	0.57
Cre4-2	40	0.32	0.164*	0.67	0.48
Cre4-3	39	0.29	0.093*	0.71	0.00
Cre4-4	39	0.28	0.121*	0.13	0.00
Cre4-5	37	0.28	0.088*	0.68	0.51
Cre4-6	38	0.30	0.037	.	.
Cre4-7	39	0.30	0.205*	0.00	0.76
Cre4-8	38	0.26	0.142*	0.72	0.48
Cre4-9	40	0.28	0.114*	0.07	0.17
Den3-1	39	0.31	0.055	.	.
Den3-2	39	0.35	0.145*	0.60	0.75
Den3-3	36	0.33	0.112*	0.11	0.00
Den3-4	36	0.31	0.077	.	.
Den3-5	37	0.32	-0.033	.	.
Den3-6	40	0.34	0.056	.	.
Den3-7	39	0.36	0.158*	0.64	0.38
Den3-8	40	0.34	0.161*	0.05	0.43

Den3-9	40	0.35	0.066	.	.
Den3-10	39	0.39	0.000	.	.

540

541

542 **Figure 1 – Esquibet *et al.***

543

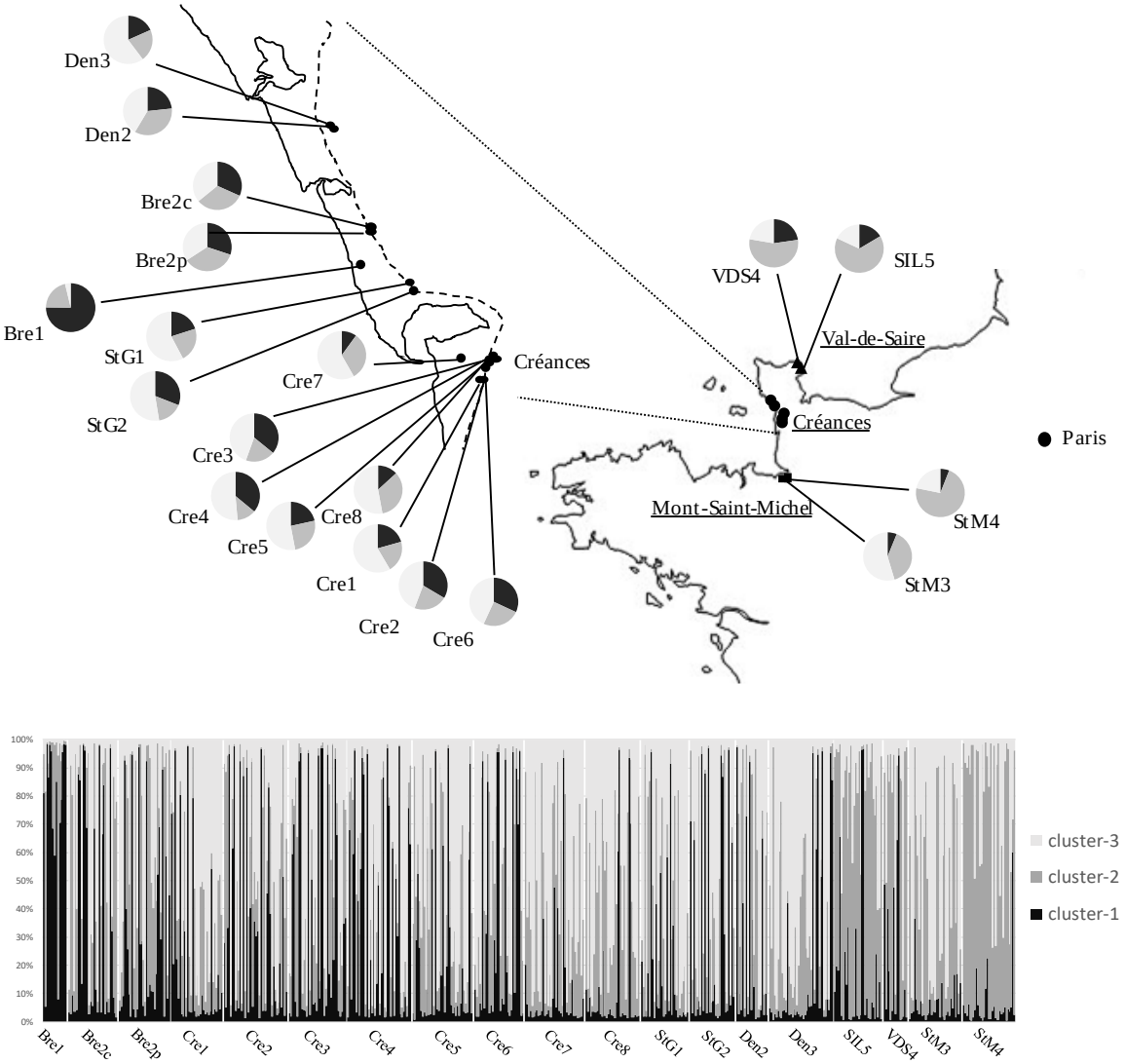

544

545

546

547 **Figure 2 – Esquibet *et al.***

548

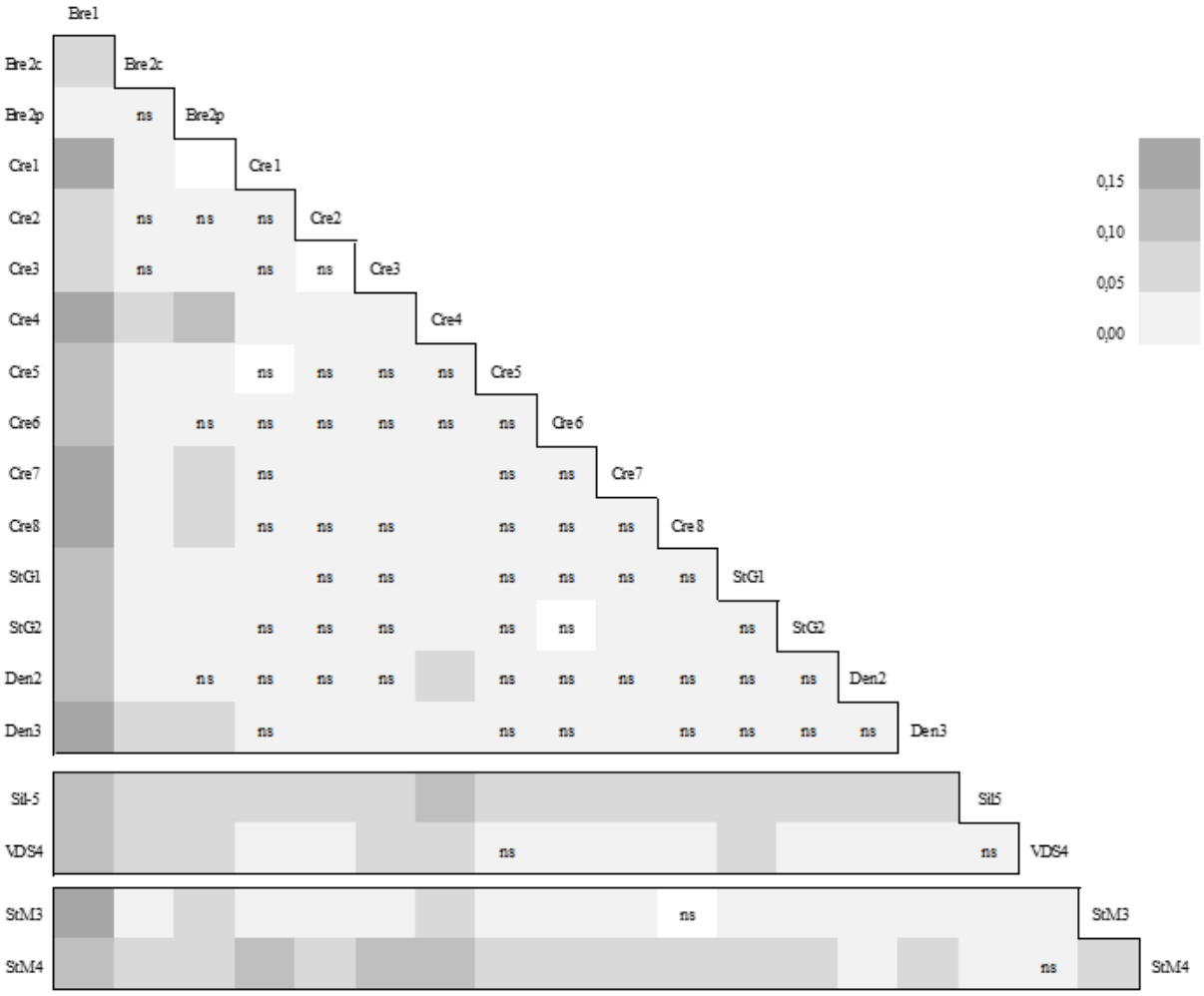

549

550

551 **Figure 3 – Esquibet *et al.***

552

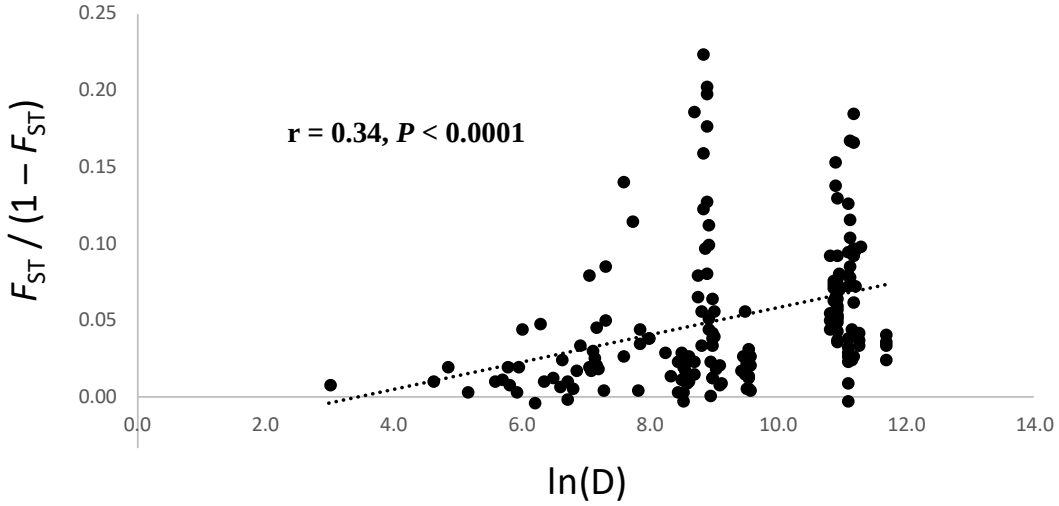

553

554

Figure S1 – Esquibet *et al.*

Factorial correspondence analysis (FCA) performed on the 822 individuals collected at the field scale (circles). The 114 individuals which formed a distinct group (black circles) from all the other individuals (grey circles), were clearly grouped with the 64 *H. cruciferae* individuals coming from two reference populations (white triangles). All the other individuals were clearly grouped with the 36 individuals from the two reference *H. carotae* populations (white squares). The two first axes explained 22% and 3.5% of the genetic variability, respectively.

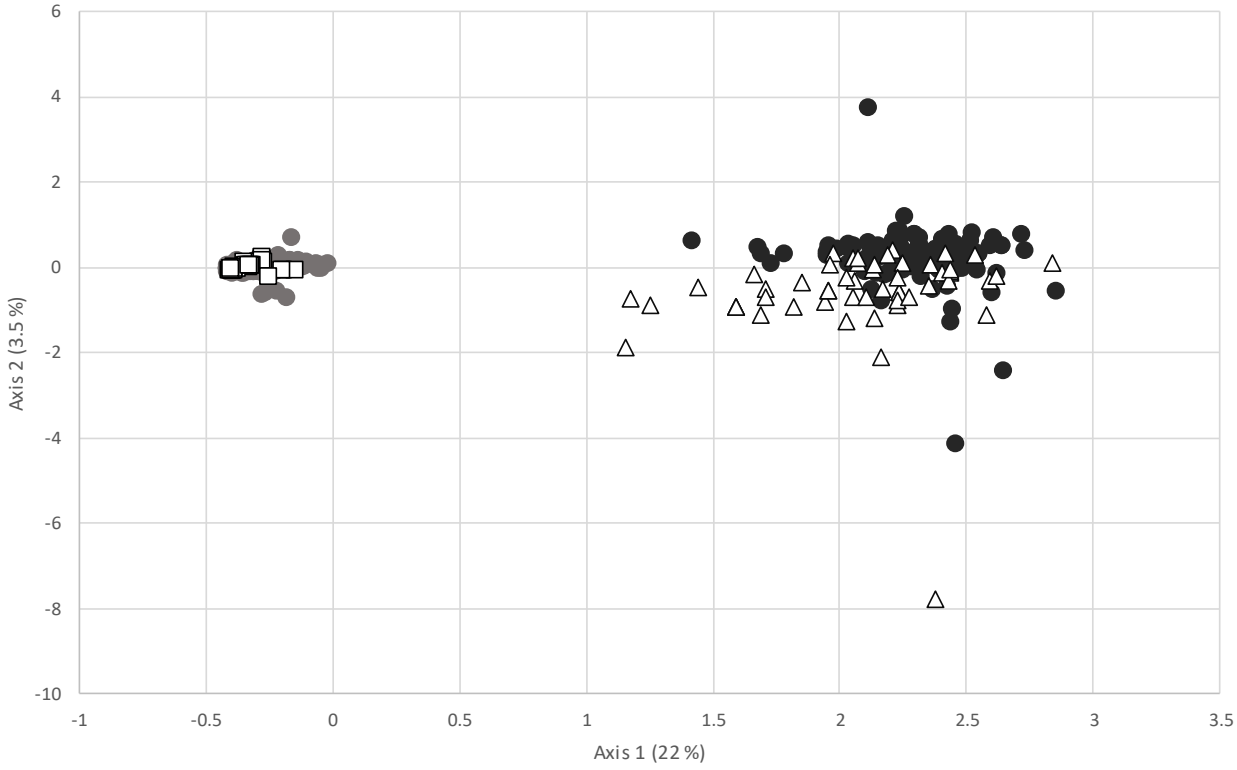

Figure S2 – Esquibet *et al.*

Likelihood surfaces showing estimated θ and C values with 95 and 99% confidence envelopes for the 12 *H. carotae* populations sampled at the spatial scale of the plant showing significant heterozygote deficits (eight populations from the field Cre4 and four populations from the field Den3).